Supporting information

Compensated second-order recoupling: application to Third Spin Assisted Recoupling

Mathilde Giffard,[a] Sabine Hediger,[a] Józef R. Lewandowski,[b] Michel Bardet,[a] Jean-Pierre Simorre,[c] Robert G. Griffin[d] and Gaël De Paëpe[a*]

Section 1

a- Analytical expression of the TSAR effective coupling:

The analytical expression of the TSAR effective frequency (for the solution $p_A=p_B$) is given by the following expression:[1]

$$\omega^{\mathrm{TSAR}}_{ZQ,\delta p_0} = \left(\frac{\mathrm{Re}\left(\omega^{1}_{AH}\ \omega^{-1}_{HB}\right)}{\omega_r}\lambda(1,p_A,p_H)+\frac{\mathrm{Re}\left(\omega^{2}_{AH}\ \omega^{-2}_{HB}\right)}{\omega_r}\lambda(2,p_A,p_H)\right) + i\left(\frac{\mathrm{Im}\left(\omega^{1}_{AH}\ \omega^{-1}_{HB}\right)}{\omega_r}\sigma(1,p_A,p_H)+\frac{\mathrm{Im}\left(\omega^{2}_{AH}\ \omega^{-2}_{HB}\right)}{\omega_r}\sigma(2,p_A,p_H)\right) \quad (1)$$

with

$$\lambda(m,p_C,p_H)=\left(\frac{-(p_C+p_H)}{m^2-(p_C+p_H)^2}+\frac{-(p_H-p_C)}{m^2-(p_H-p_C)^2}\right)$$
$$\sigma(m,p_C,p_H)=\left(\frac{m}{m^2-(p_H+p_C)^2}-\frac{m}{m^2-(p_H-p_C)^2}\right) \quad (2)$$

b- ZQ fictitious spin operators involving spins k and l:

$$I^{(23)}_{kl,x}=\frac{1}{2}\left(2I_{kx}I_{lx}+2I_{ky}I_{ly}\right)=\frac{1}{2}\left(I^{+}_{k}I^{-}_{l}+I^{-}_{k}I^{+}_{l}\right)=-\left(T^{k}_{11}T^{l}_{1-1}+T^{k}_{1-1}T^{l}_{11}\right)$$
$$I^{(23)}_{kl,y}=\frac{1}{2}\left(2I_{ky}I_{lx}-2I_{kx}I_{ly}\right)=\frac{i}{2}\left(-I^{+}_{k}I^{-}_{l}+I^{-}_{k}I^{+}_{l}\right)=i\left(T^{k}_{11}T^{l}_{1-1}-T^{k}_{1-1}T^{l}_{11}\right)$$
$$I^{(23)}_{kl,z}=\frac{1}{2}\left(I_{kz}-I_{lz}\right)=\frac{1}{2}\left(T^{k}_{10}-T^{l}_{10}\right) \quad (3)$$

Section 2 – TSAR polarization transfer maps

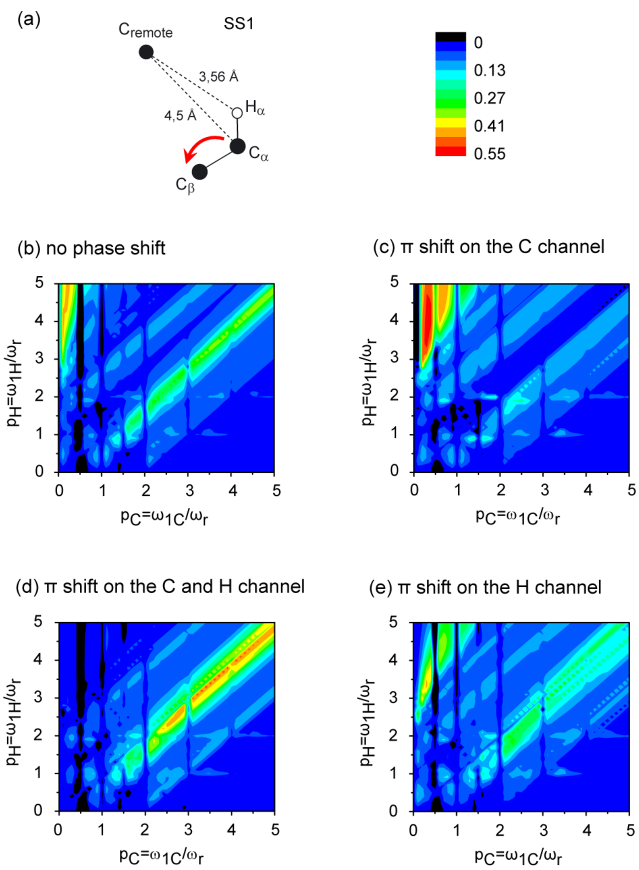

Figure SI 1. Numerical simulations of the TSAR-based polarization-transfer efficiency with and without phase shift at $\omega_{0H}/2\pi$ = 400 MHz and $\omega_r/2\pi$ = 20 kHz. The magnetization starts on the C_α spin and is detected on the directly bounded C_β spin after 5 ms of mixing time. (a) Spin system used in the simulations. (b)-(e) 2D maps of the polarization-transfer efficiency as a function of the carbon p_C and proton p_H RF-field strengths for (b) PAR, (c) *C*-PS-PAR, (d) *CH*-PS-PAR, (e) *H*-PS-PAR. The corresponding polarization transfer to the remote spin is presented in Figure 3.

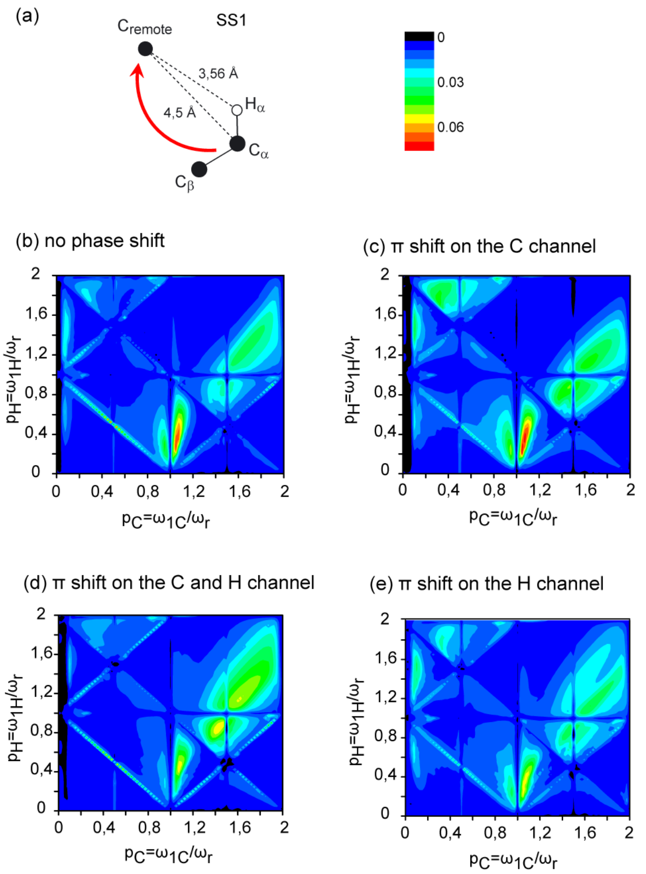

Figure SI 2. Numerical simulations of the TSAR-based polarization-transfer efficiency with and without phase shift at $\omega_{0H}/2\pi$ = 900 MHz and $\omega_r/2\pi$ = 60 kHz. The magnetization starts on the C_α spin and is detected on the C_{remote} spin after 5 ms of mixing time. (a) Spin system used in the simulations. (b)-(e) 2D maps of the polarization-transfer efficiency as a function of the carbon p_C and proton p_H RF-field strengths (expressed in units of the spinning frequency) for (b) PAR, (c) *C*-PS-PAR, (d) *CH*-PS-PAR, (e) *H*-PS-PAR. The corresponding polarization transfer to the directly bonded C_β spin is presented in Figure 5.

1. G. De Paepe, J. R. Lewandowski, A. Loquet, A. Bockmann and R. G. Griffin, *Journal of Chemical Physics*, 2008, **129**.

